

Microtubule Elasticity: Connecting All-Atom Simulations with Continuum Mechanics

David Sept^{1,*} and Fred C. MacKintosh^{2,†}

¹*Department of Biomedical Engineering and Center for Computational Medicine and Bioinformatics, University of Michigan, Ann Arbor, Michigan 48109, USA*

²*Department of Physics and Astronomy, Vrije Universiteit, 1081 HV Amsterdam, The Netherlands*
(Received 9 November 2009; published 4 January 2010)

The mechanical properties of microtubules have been extensively studied using a wide range of biophysical techniques, seeking to understand the mechanics of these cylindrical polymers. Here we develop a method for connecting all-atom molecular dynamics simulations with continuum mechanics and show how this can be applied to understand microtubule mechanics. Our coarse-graining technique applied to the microscopic simulation system yields consistent predictions for the Young's modulus and persistence length of microtubules, while clearly demonstrating how binding of the drug Taxol decreases the stiffness of microtubules. The techniques we develop should be widely applicable to other macromolecular systems.

DOI: [10.1103/PhysRevLett.104.018101](https://doi.org/10.1103/PhysRevLett.104.018101)

PACS numbers: 87.16.Ka, 83.10.-y, 87.15.A-, 87.15.La

Microtubules are essential players in a wide range of cellular functions. The protein tubulin polymerizes to form these filaments resulting in a hollow cylinder with a diameter of about 25 nm and lengths that range from tens of nanometers to tens of microns. Microtubules are the most rigid structures within the cell and their mechanical stability is particularly important for the role that microtubules play in cell division, cellular transport, and their basic ability to help provide cell shape. The mechanical properties of purified microtubules have been studied extensively using many biophysical techniques, including atomic force microscopy, thermal bending, and single molecule techniques [1–11]. Since microtubules are dynamic polymers and have intrinsic instability, many of these experimental studies have been performed on Taxol-stabilized microtubules, although the mechanical consequences of the drug Taxol for microtubule mechanics remains unclear. The majority of studies have found that the addition of Taxol results in “softer” microtubules with a shorter persistence length and lower Young's modulus [1–5], while one published study had found the opposite result [6]. Recently, even the standard elastic model of microtubules characterized by a single elastic bending constant has been called into question by reports of length-dependent stiffness [12]. Thus, in spite of decades of experimental study, many basic questions and puzzles remain concerning the mechanics of even individual microtubules *in vitro*, let alone *in vivo*.

Here, we combine all-atom simulations and continuum elastic modeling in order to determine both the elastic parameters of persistence length and Young's modulus, as well as to test the applicability of simple, continuum shell elasticity for microtubules. Based on a molecular dynamics simulation of a small section of six tubulin monomers [13], we show that the observed fluctuations of this section are consistent with linear elastic constants for both bending and stretching along the microtubule axis.

From these measurements, we determine the effective elastic properties for the microtubule wall, treated as an elastic sheet. With the addition of Taxol, we find increased flexibility and reduced bending and stretching moduli. We then examine the shear strain fluctuations of the tubulin sheet and find evidence for enhanced shear compliance, relative to the predictions of homogenous and isotropic elasticity. While anomalously large shear compliance has been suggested recently in connection with length-dependent bending stiffness of microtubules [12], we find a much smaller degree of anisotropy than previously suggested. The shear elasticity we find is closer to recent experiments [9].

We base our atomistic simulations on known tubulin structure. The atomic structure of the tubulin dimer was first solved as a result of ground-breaking electron microscopy work on tubulin sheets [14]. An 8 Å structure of the microtubule was solved in subsequent work, and the combination of these two pieces resulted in a molecular level model of microtubule [15]. Using this structure, we performed all-atom molecular dynamics simulations on a fragment of a microtubule with and without Taxol [13]. These were explicit solvent simulations performed using a six monomer portion of two neighboring protofilaments (Fig. 1). The total simulation time for both the Taxol-free and Taxol-bound systems was 30 ns; however, analysis was only performed on the last 25 ns to allow for equilibration. Simulations were performed using NAMD [16], and importantly no constraints were applied to the system to help maintain the integrity of the protofilament structure. These simulations revealed many interesting features of the microtubule structure and its dynamics, most notably that the addition of Taxol increases the flexibility of the dimer-dimer interface along the protofilament. Based on this finding, we felt that this increase in flexibility should manifest itself at the level of the polymer and we sought

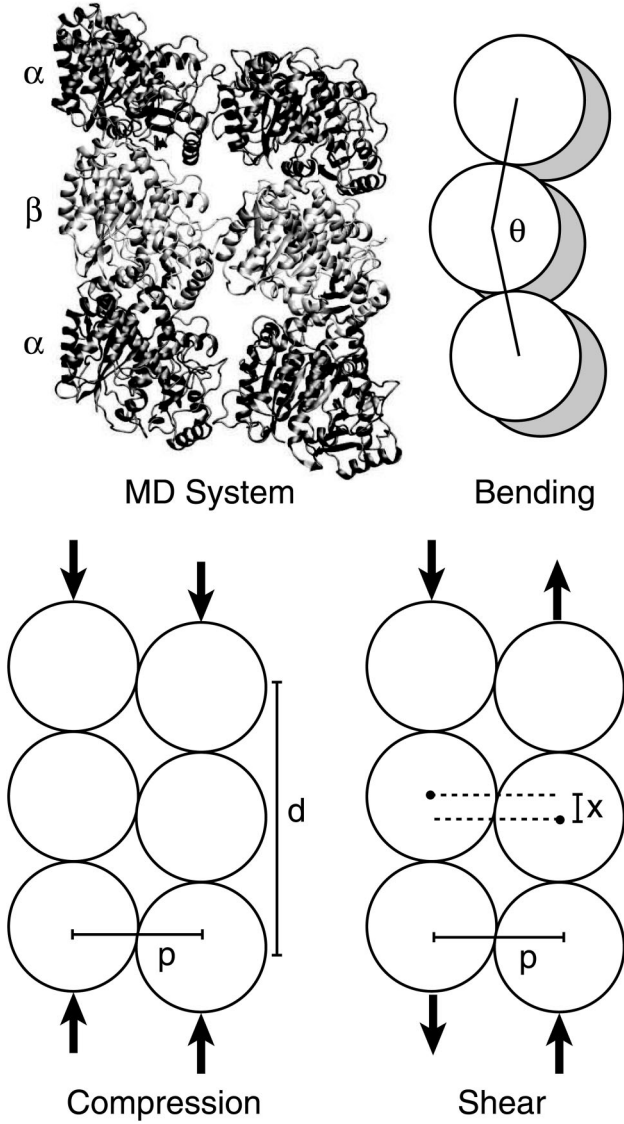


FIG. 1. A depiction of the all-atom simulations system and the bending, compression, and shear modes we capture in our coarse-grained model.

a method to connect our microscopic simulations and with macroscopic experimental results.

As sketched in Fig. 1, we coarse-grained our atomic level model by replacing each tubulin monomer with a bead placed at the center of mass of the monomer. With this simplification, our molecular dynamics simulation is reduced to the dynamics of six individual beads, and by tracking the relative motion of these beads we can extract motions that correspond to bending, compression, and shear modes (see Fig. 1). Most often mechanical properties are elucidated in experiments by calculating a force-displacement curve as the system is subjected to an applied force. Our simulations were performed as equilibrium molecular dynamics simulations [13] and did not include such a force; however, we can make use of the equipartition theorem and knowledge of the energy involved in the bending, compression or shear of a sheet, assuming a

harmonic dependence. In the case of bending, the elastic energy can be described by the bending rigidity κ of an elastic shell formed by the protofilaments, according to

$$\langle E_{\text{bend}} \rangle = \frac{kT}{2} = \frac{2p}{d} \kappa \langle \theta^2 \rangle, \quad (1)$$

where $kT/2$ is the thermal energy set by the simulation temperature, d is the dimer repeat length, $2p$ is the width of the two protofilaments, and θ is the measure bending angle. The values for the dimer length and protofilament width were determined from our atomic model as $d = 8.4$ nm and $p = 5.2$ nm. Similarly for the compression mode we find

$$\langle E_{\text{comp}} \rangle = \frac{kT}{2} = \frac{p}{d} E^{(2D)} \langle \Delta d^2 \rangle, \quad (2)$$

where $E^{(2D)}$ is the 2D Young's modulus and $\epsilon = \Delta d/d$ is the measured strain. Finally, the shear is determined from fluctuations $\Delta x = x - \langle x \rangle$ in the offset x between the protofilaments:

$$\langle E_{\text{shear}} \rangle = \frac{kT}{2} = \frac{3d}{4p} G^{(2D)} \langle \Delta x^2 \rangle \quad (3)$$

where $G^{(2D)}$ is the 2D shear modulus and $\gamma = \Delta x/p$ is the shear strain. The distributions obtained from the simulations were fit well by Gaussians (Fig. 2), from which we obtained the 2D bending, Young's, and shear moduli for both the apo (no Taxol) and Taxol-bound cases using Eqs. (1)–(3).

These 2D moduli are for the portion of the microtubule wall in our simulation system, although we wish to connect them to elastic parameters for the full microtubule. To do this we make use thin shell mechanics. If we assume the microtubule to be an isotropic, thin cylindrical shell of thickness h , we know that

$$\kappa = \frac{Eh^3}{12[1 - \nu^2]}, \quad E^{(2D)} = Eh, \quad \text{and} \quad G^{(2D)} = Gh, \quad (4)$$

where ν is Poisson's ratio and E and G are 3D moduli. If we assume a value for ν of 0.3, consistent with materials such as nylon, we get Young's moduli of 2.2 and 0.38 GPa and shear moduli of 47 and 48 MPa for the apo and Taxol microtubule, respectively (see Table I). These values are in good agreement with experimental measurements, both in terms of the order of magnitude and the fact that the Taxol microtubule has a lower Young's modulus. The effective shell thickness h that results from these calculations is also in line with the real thickness of the microtubule wall. Further, since we know the moment of inertia (per unit length and mass density) for a cylinder is $I = \frac{\pi}{4}(r_{\text{outer}}^4 - r_{\text{inner}}^4)$, we can calculate the corresponding persistence length as

$$\ell_p = \frac{EI}{kT}. \quad (5)$$

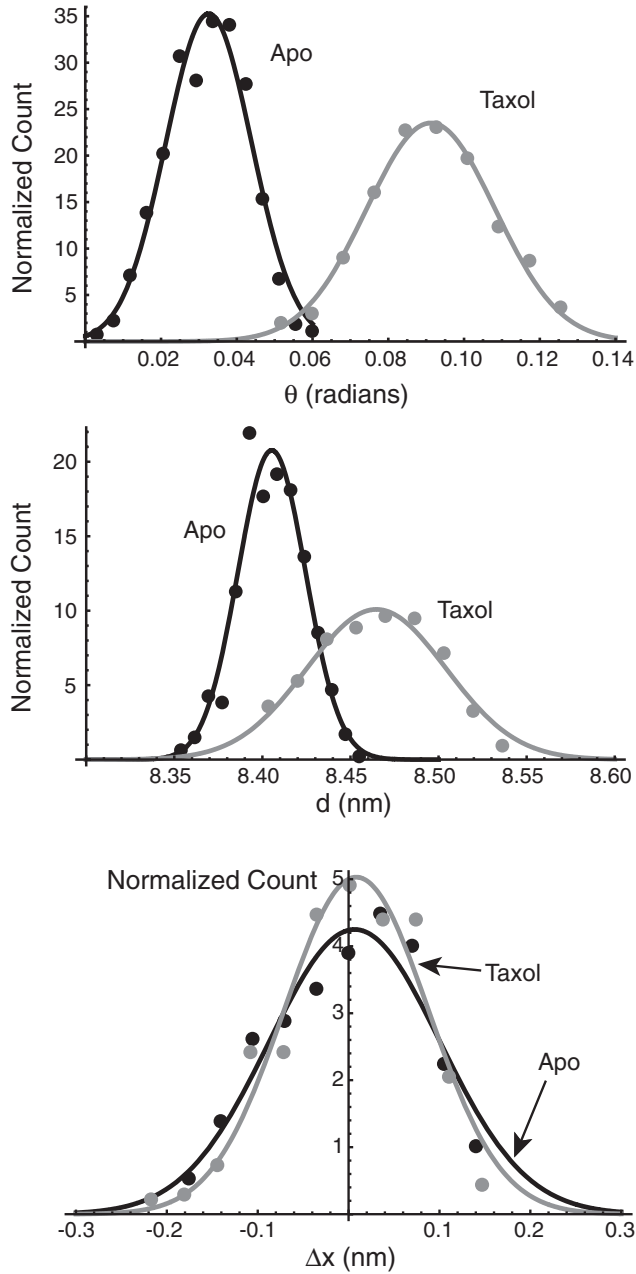


FIG. 2. The observed angle (top), contour length (middle), and offset (bottom) distributions from the molecular dynamics simulations. The black points are from the Taxol-free or apo simulations, the gray points are from the Taxol simulations, and the lines represent best fit Gaussians to each set of simulations.

Putting in 12 and 8 nm for the outer and inner radii of the microtubule [15], we get $\ell_p = 6.9$ mm for the apo microtubule and 1.2 mm for the Taxol microtubule. All of these parameters are summarized in Table I.

Apart from the differences in bending rigidity, it is interesting to note the differences in the mean angle and dimer spacing between the apo and Taxol simulations. Although the difference in the mean bending angle is small, the Taxol system does appear to adopt a slightly more bent conformation. Experiments have found the con-

TABLE I. Mechanical parameters determined from our simulations for apo and Taxol microtubules. Experimental values for E were taken from [7,10] and calculated from measured values of the bending rigidity EI using our value for I [1–3,8]. Experimental values for G are from [9,17], and values for ℓ_p are taken from [3] using Eq. (5) and the experimental values for the bending rigidity cited above. Values for h are taken from structural data in Ref. [15].

	Apo		Taxol	
	MD	Experiment	MD	Experiment
κ ($\times 10^4$ pN nm ²)	1.25		0.56	
$E^{(2D)}$ ($\times 10^4$ pN/nm)	8.73		2.06	
$G^{(2D)}$ (pN/nm)	187		262	
E (GPa)	2.2	0.33–1.3	0.38	0.13–0.17
G (MPa)	47	1.4–12	48	
h (nm)	4.0	4.0	5.4	4.0
ℓ_p (mm)	6.9	1.1–2.2	1.2	0.5–1.2

trary result where individual protofilaments stabilized with Taxol appear more straight than those only with a non-hydrolyzable analog of guanosine triphosphate [18]. Our simulations are certainly limited by the relatively small size of the system, and the bend angles may indeed be different from the angles we would observe between two dimers. The dimer-dimer spacing along the protofilament d shows interesting differences between the two simulations. In the presence of Taxol, the spacing is increased slightly by about 1 Å, and this effect has been observed experimentally where the monomer-monomer spacing along the protofilament changes in the presence of Taxol [19,20].

Since the microtubule is constructed from discrete protofilaments, it is not obvious that a model of the microtubule wall as an isotropic, continuum elastic sheet is a good one, although some recent experiments have suggested this [10,11]. By contrast, it has also recently been suggested that there are very strong anisotropy effects, specifically in the form of a very soft bend [21] and shear [12] elasticity between adjacent protofilaments. Some anisotropy is to be expected, given the protofilament structure. Our combined observations of bending, compression, and especially shear provide a test of this. We find, for instance, that the implied shear modulus G corresponding to interprotofilament sliding is much smaller than the Young's modulus E corresponding to axial compression of the protofilaments. This cannot be accounted for by isotropic elasticity where one would expect $E = 2G(1 + \nu)$. However, we find that the shear moduli for both apo and Taxol-stabilized microtubules are only about an order of magnitude smaller than the corresponding Young's moduli, in contrast with the approximately 6 orders of magnitude suggested by the model in Ref. [12], which suggested a value for G of order 1 kPa. Our results for the shear modulus are much closer to subsequent measurements of Kis *et al.* [17], who report G in the range of 2–12 MPa. Thus, while there are indications of anisotropy in our

simulations, the degree of anisotropy we observe is not sufficient to account for the apparent length-dependent stiffness of microtubules in Ref. [12]. It has been suggested that the apparent length dependence may be accounted for by the enhanced relative noise in measuring small amplitude bending fluctuations [22]. Concerning the possibility of enhanced interprotofilament bending, we note that, although we find only an approximate tenfold enhancement of shear compliance between filaments, the protofilament structure provides a possible explanation for the much larger compliance for interprotofilament bending observed in Ref. [21]: the bending of a shell depends much more sensitively on the shell thickness than does the shear. Thus, given the known thinning of the microtubule structure at the interface between protofilaments, a greatly enhanced azimuthal bending compliance can be expected. Interestingly, if this is the origin of the bending observed by Needleman *et al.* [21], our finding of a very weak effect of Taxol on shear could provide an explanation of their report of no Taxol dependence. By contrast, as discussed in Refs. [10,11], pointlike forces applied, e.g., by an atomic force microscopy tip result in significant interprotofilament shear and axial stretching. Thus, a much weaker effect of the riblike protofilament structure is expected for such experiments.

Although we have limited our focus to the microtubule, these techniques should be widely applicable to other macromolecular systems. Other studies have used molecular mechanics techniques to perform tensile tests on the tubulin monomer [23], and more complete studies using hybrid molecular dynamics or finite element modeling have been applied to study mechanosensitive ion channels [24]. The coarse-graining techniques developed here are similar to a large number of bead-spring models that have been developed to describe biomolecular systems (see [25] for a nice summary of current approaches). Similar to our case, these approaches use particles to represent one or more atoms in the system and then apply harmonic or other effective potentials to describe the interaction between the particles. The application of the techniques described here to other systems should be relatively straightforward, provided one is able to identify the basic structural units within the larger macromolecular complex. In the case of biological polymers such as actin filaments or DNA there is a clear means of achieving this; however, for more complicated complexes or system such as biomembranes, more work may be required.

D.S. was supported in part by the NSF (Grant No. CMMI-0928540). F.M. was supported by FOM/NWO. We thank the Aspen Center for Physics, where this work was initially conceived and implemented. We also thank A.E. Carlsson and C.F. Schmidt for helpful discussions.

*dsept@umich.edu

†fcm@nat.vu.nl

- [1] M. Kikumoto, M. Kurachi, V. Tosa, and H. Tashiro, *Biophys. J.* **90**, 1687 (2006).
- [2] H. Felgner, R. Frank, and M. Schliwa, *J. Cell Sci.* **109**, 509 (1996).
- [3] P. Venier, A. C. Maggs, M. F. Carlier, and D. Pantaloni, *J. Biol. Chem.* **269**, 13 353 (1994).
- [4] R. B. Dye, S. P. Fink, and R. C. Williams, *J. Biol. Chem.* **268**, 6847 (1993).
- [5] M. Kurachi, M. Hoshi, and H. Tashiro, *Cell Motil. Cytoskeleton* **30**, 221 (1995).
- [6] B. Mickey and J. Howard, *J. Cell Biol.* **130**, 909 (1995).
- [7] D. J. Needleman, M. A. Ojeda-Lopez, U. Raviv, K. Ewert, H. P. Miller, L. Wilson, and C. R. Safinya, *Biophys. J.* **89**, 3410 (2005).
- [8] K. Kawaguchi, S. Ishiwata, and T. Yamashita, *Biochem. Biophys. Res. Commun.* **366**, 637 (2008).
- [9] A. Kis, S. Kasas, B. Babic, A. J. Kulik, W. Benoit, G. A. D. Briggs, C. Schonenberger, S. Catsicas, and L. Forro, *Phys. Rev. Lett.* **89**, 248101 (2002).
- [10] P. J. de Pablo, I. A. T. Schaap, F. C. MacKintosh, and C. F. Schmidt, *Phys. Rev. Lett.* **91**, 098101 (2003).
- [11] I. A. T. Schaap, C. Carrasco, P. J. de Pablo, F. C. MacKintosh, and C. F. Schmidt, *Biophys. J.* **91**, 1521 (2006).
- [12] F. Pampaloni, G. Lattanzi, A. Jonas, T. Surrey, E. Frey, and E. L. Florin, *Proc. Natl. Acad. Sci. U.S.A.* **103**, 10248 (2006).
- [13] A. Mitra and D. Sept, *Biophys. J.* **95**, 3252 (2008).
- [14] E. Nogales, S. G. Wolf, and K. H. Downing, *Nature (London)* **391**, 199 (1998).
- [15] H. Li, D. J. DeRosier, W. V. Nicholson, E. Nogales, and K. H. Downing, *Structure* **10**, 1317 (2002).
- [16] L. Kale, R. Skeel, M. Bhandarkar, R. Brunner, A. Gursoy, N. Krawetz, J. Phillips, A. Shinozaki, K. Varadarajan, and K. Schulten, *J. Comput. Phys.* **151**, 283 (1999).
- [17] A. Kis, S. Kasas, A. J. Kulik, S. Catsicas, and L. Forro, *Langmuir* **24**, 6176 (2008).
- [18] C. Elie-Caille, F. Severin, J. Helenius, J. Howard, D. J. Muller, and A. A. Hyman, *Curr. Biol.* **17**, 1765 (2007).
- [19] R. D. Vale, C. M. Coppin, F. Malik, F. J. Kull, and R. A. Milligan, *J. Biol. Chem.* **269**, 23 769 (1994).
- [20] I. Arnal and R. H. Wade, *Curr. Biol.* **5**, 900 (1995).
- [21] D. J. Needleman, M. A. Ojeda-Lopez, U. Raviv, K. Ewert, J. B. Jones, H. P. Miller, L. Wilson, and C. R. Safinya, *Phys. Rev. Lett.* **93**, 198104 (2004).
- [22] C. P. Brangwynne, G. H. Koenderink, E. Barry, Z. Dogic, F. C. MacKintosh, and D. A. Weitz, *Biophys. J.* **93**, 346 (2007).
- [23] A. S. Zeiger and B. E. Layton, *Biophys. J.* **95**, 3606 (2008).
- [24] X. Chen, Q. Cui, Y. Tang, J. Yoo, and A. Yethiraj, *Biophys. J.* **95**, 563 (2008).
- [25] G. A. Voth, *Coarse-Graining of Condensed Phase and Biomolecular Systems* (CRC Press, Boca Raton, 2009).